

Preparation and Crystal Structure of $\text{Tl}_3\text{Al}_{13}\text{S}_{21}$, A Novel Ternary Sulfide Structure Type

Bernt Krebs* and Horst Greiwing

Institute of Inorganic Chemistry, University of Münster, Wilhelm-Klemm-Strasse 8, D-4400 Münster, Germany

Krebs, B. and Greiwing, H., 1991. Preparation and Crystal Structure of $\text{Tl}_3\text{Al}_{13}\text{S}_{21}$, A Novel Ternary Sulfide Structure Type. – Acta Chem. Scand. 45: 833–839.

Light-yellow single crystals of $\text{Tl}_3\text{Al}_{13}\text{S}_{21}$ were grown from a stoichiometric mixture of the binary compounds Tl_2S and Al_2S_3 at 1000–1050 K in evacuated silica tubes. The title compound crystallizes in the monoclinic space group Cm with $a = 25.242(5)$, $b = 14.900(3)$, $c = 9.259(1)$ Å, $\beta = 103.81(1)^\circ$ and $Z = 4$. The structure was determined from single-crystal X-ray diffraction data and was refined to final R and R_w indices of 0.056 and 0.053, respectively. In this new tetrahedral structure type slightly distorted AlS_4 tetrahedra (Al–S 2.177–2.329 Å) are connected via common corners, forming a polymeric, largely covalent, three-dimensional framework. There is a layer-like ...AABAAB... ordering perpendicular to c of this tetrahedral arrangement. The Tl atoms are located in tunnels along [001], with their coordination by 12, 11 or 9 sulfur atoms being rather irregular owing to the stereochemical activity of the lone electron pair (Tl–S 3.109–3.974 Å). The structure can be described as containing a distorted close packing of 21 S + 3 Tl per formula unit, with an ordered occupation of 13 of the tetrahedral voids by Al.

Dedicated to Professor Sten Andersson on the occasion of his 60th birthday.

Studies of ternary systems based on aluminium sulfide have mainly been undertaken with respect to the structural chemistry of new phases, but they have also been stimulated by prospects for possible interesting physical properties such as electrical conductivities and ion-transport properties for use as solid electrolytes.¹ Up to now only a limited number of ternary phases in the aluminium–sulfur system (mainly chalcopyrite-type and spinel-type phases) have been published and fully characterized by complete single-crystal structure determinations. The reasons for these deficiencies are probably experimental problems in the preparation of pure phases that arise because of the inherent instability of the Al–S bond towards reaction with oxygen or towards hydrolysis, and consequently certain problems in their reactivity towards container materials such as silica glass. In our preparative and structural investigations on ternary aluminium chalcogenides we were interested in stereochemical aspects of the metal–chalcogen framework and in the structural influence of lone-pair electrons, especially of main-group elements. This, as well as the large structural variety found in other ternary thallium–sulfur systems with B, Si, Ge and Sn (e.g. Refs. 2–8) indicated the $\text{Tl}_2\text{S}/\text{Al}_2\text{S}_3$ phase system to be especially interesting.

So far TlAlS_2 appears to be the only phase having been characterized in this ternary system. It crystallizes in the

TlGaSe_2 structure type,^{9–11} which consists of layers of corner-sharing adamantane-like $[\text{M}_4\text{X}_{10}]$ super-tetrahedra ($\text{M} = \text{Ga}, \text{Al}; \text{X} = \text{S}, \text{Se}$); the Tl^+ ions in the interlayer space are irregularly coordinated.

Interesting structures in other ternary aluminium–sulfur systems are to be found in the $\text{BaS}/\text{Al}_2\text{S}_3$ system. BaAl_2S_4 ¹² crystallizes in a unique structure type where corner-sharing $[\text{AlS}_4]$ tetrahedra form a three-dimensional framework with 6- and 14-membered Al–S rings. BaAl_4S_7 ¹³ consists of corner-sharing $[\text{AlS}_4]$ tetrahedra connected to 6-, 8- and 12-membered Al–S rings, leading to a three-dimensional network with wide voids in which the Ba^{2+} ions are located. Both barium thioaluminates contain structural features that also appear in the structure of $\text{Tl}_3\text{Al}_{13}\text{S}_{21}$, the preparation and structure of which will be discussed in this paper.

Experimental

Synthesis. Light-yellow plate-shaped crystals of $\text{Tl}_3\text{Al}_{13}\text{S}_{21}$ were obtained from a stoichiometric mixture of the high-purity binary compounds Tl_2S and Al_2S_3 . Tl_2S was prepared by fusing stoichiometric mixtures of the elements in evacuated Pyrex glass tubes at 730 K for 1 day followed by a 4 day period of annealing at 520 K (thallium shot, 99.995 % Alfa, sulfur powder, DAB 6, Merck). Al_2S_3 was made by chemical vapour transport with iodine in evacuated silica tubes at 1130–1020 K (aluminium foil, 99.96 %, Merck).

* To whom correspondence should be addressed.

Table 1. Crystal data for $\text{Ti}_3\text{Al}_{13}\text{S}_{21}$.

Formula	$\text{Ti}_3\text{Al}_{13}\text{S}_{21}$
Molecular weight/g mol ⁻¹	1637.22
Space group	<i>Cm</i> (No. 8)
Cell parameters (295 K)	
<i>a</i> /Å	25.242(5)
<i>b</i> /Å	14.900(3)
<i>c</i> /Å	9.259(1)
β /°	103.81(1)
<i>V</i> /Å ³	3382(1)
Calculated density (295 K)/g cm ⁻³	3.216
Formula units per cell	4
Crystal size/mm ³	0.05×0.12×0.15
Radiation (Mo <i>K</i> α), λ/Å	0.71073
Linear absorption coefficient, μ/mm ⁻¹	16.0
Absorption correction, empirical	ψ-scan
Scan mode	θ-2θ
Scan speed (variable)/min ⁻¹	2.09-14.65
2θ limits/°	4-56
No. of unique data	4358
No. of data with $I/\sigma(I) \geq 2$	2799
No. of variables	353
$R = \sum(F_o - F_c) / \sum F_o $	0.056
$R_w = [\sum w(F_o - F_c)^2 / \sum w F_o ^2]^{1/2}$	0.053

The purity of both binary compounds was checked by X-ray powder diffraction diagrams. Ti_2S and Al_2S_3 , as well as $\text{Ti}_3\text{Al}_{13}\text{S}_{21}$, were manipulated exclusively in dry-nitrogen glove boxes. The reaction mixture was carefully powdered and sealed under vacuum in specially prepared silica tubes. The surface of these silica tubes was protected because of a possible aluminium-silicon exchange reaction (cf. the corresponding reaction with boron-sulfur compounds)² by a tight layer of glassy carbon created by anaerobic pyrolysis of acetone vapour. The sample was slowly heated to the reaction temperature of 1000-1050 K, then annealed at this temperature for 21 days and finally quenched to room temperature. The reaction tube contained a light-yellow crystal powder with small plate-shaped single crystals that were very sensitive to moisture. The absence of a sintered regulus indicated that the reaction might be a purely solid-state one.

Crystal structure determination. The complete crystal structure of $\text{Ti}_3\text{Al}_{13}\text{S}_{21}$ was determined from single-crystal X-ray diffraction data. Intensity data were collected on a Siemens R3 automatic diffractometer at room temperature. The cell constants were determined by least-squares refinement from diffractometer coordinates of 24 medium-angle reflections. The structure was solved by direct statistical methods of phase determination using the SHELXTL PLUS program system on a DEC VAX cluster. The structure was refined by full-matrix least-squares minimization of $\sum w(|F_o| - |F_c|)^2$.

Owing to difficulties in determining all heavy-atom positions, the structure was first solved in the centrosymmetric space group *C2/m* and then transformed to *Cm*. Sub-

Table 2. Positional parameters and isotropic thermal parameters (Å²) for $\text{Ti}_3\text{Al}_{13}\text{S}_{21}$.

Atom	<i>x</i>	<i>y</i>	<i>z</i>	U_{eq}^a
Ti(1)	0.11343	0.0000	0.0358	0.0561(10)
Ti(2)	0.18200(13)	0.0000	0.6229(3)	0.0616(11)
Ti(3)	0.57864(11)	0.0000	0.3752(3)	0.0605(10)
Ti(4)	0.44990(10)	0.0000	0.7159(3)	0.0548(9)
Ti(5)	0.88700(10)	0.0000	0.9662(3)	0.0516(9)
Ti(6)	0.81822(12)	0.0000	0.3975(3)	0.0590(10)
S(1)	0.0791(4)	0.0000	0.3598(10)	0.026(4)
S(2)	0.6969(3)	0.1172(6)	0.3779(7)	0.030(3)
S(3)	0.9527(3)	0.1320(6)	0.3743(7)	0.028(3)
S(4)	0.2013(3)	0.1226(6)	0.3526(8)	0.029(3)
S(5)	0.4570(3)	0.1145(6)	0.3843(7)	0.029(3)
S(6)	0.6347(4)	0.0000	0.0385(11)	0.024(3)
S(7)	0.5116(3)	0.1179(5)	0.0291(8)	0.026(2)
S(8)	0.0795(3)	0.2498(5)	0.3729(7)	0.026(3)
S(9)	0.1920(3)	0.2473(5)	0.7091(7)	0.021(2)
S(10)	0.6908(4)	0.0000	0.7045(10)	0.026(4)
S(11)	0.0059(3)	0.1221(5)	0.0413(7)	0.026(3)
S(12)	0.2595(3)	0.1312(6)	0.0317(7)	0.024(3)
S(13)	0.6366(3)	0.2476(5)	0.0396(8)	0.024(2)
S(14)	0.9388(4)	0.0000	0.6870(10)	0.025(4)
S(15)	0.8166(3)	0.1203(5)	0.6920(8)	0.027(3)
S(16)	0.3273(4)	0.0000	0.3676(10)	0.028(4)
S(17)	0.3222(3)	0.1207(5)	0.7040(7)	0.025(3)
S(18)	0.9424(3)	0.2461(5)	0.7093(7)	0.024(3)
S(19)	0.5665(3)	0.1215(5)	0.6938(8)	0.026(3)
S(20)	0.3887(3)	0.2478(6)	0.0457(8)	0.026(3)
S(21)	0.3308(3)	0.2489(6)	0.3731(7)	0.027(3)
S(22)	0.3844(4)	0.0000	0.0341(10)	0.020(3)
S(23)	0.7659(3)	0.1188(6)	0.0429(8)	0.030(3)
S(24)	0.0708(3)	0.1216(5)	0.7072(8)	0.024(2)
Al(1)	0.5843(3)	0.1241(6)	0.9382(8)	0.023(3)
Al(2)	0.7267(3)	0.1272(6)	0.6202(8)	0.025(3)
Al(3)	0.5976(3)	0.2491(7)	0.6289(8)	0.027(3)
Al(4)	0.6598(3)	0.2471(7)	0.2970(8)	0.027(3)
Al(5)	0.0302(3)	0.1238(6)	0.2868(9)	0.026(3)
Al(6)	0.7142(4)	0.0000	0.9588(11)	0.025(4)
Al(7)	0.7152(3)	0.2350(6)	0.9621(9)	0.027(3)
Al(8)	0.8489(3)	0.2478(6)	0.6315(8)	0.024(3)
Al(9)	0.4069(4)	0.0000	0.2862(12)	0.025(4)
Al(10)	0.2787(3)	0.1270(6)	0.2854(8)	0.026(3)
Al(11)	0.9807(3)	0.1204(6)	0.6320(8)	0.025(3)
Al(12)	0.3372(3)	0.1293(6)	0.9457(8)	0.026(3)
Al(13)	0.4694(3)	0.2469(6)	0.9658(8)	0.022(3)
Al(14)	0.4110(3)	0.2349(6)	0.3004(8)	0.021(3)

^a U_{eq} is defined as 1/3 of the trace of the orthogonalised U_{ij} tensor.

sequent difference electron density maps provided the parameters for the remaining atoms in the structure. The refinement with anisotropic temperature factors for all atoms, with atomic scattering factors for neutral atoms (including anomalous dispersion corrections), converged to a conventional *R* value of 0.056. The weighting scheme was based on the variance of the intensities I_{hkl} : $1/w = [\sigma(F_o)]^2 + (0.01|F_o|)^2$ with $\sigma(F_o) = \sigma(I)/(2|F_o|Lp)$ (*Lp*: Lorentz and polarization factor). Further details of the crystal data for $\text{Ti}_3\text{Al}_{13}\text{S}_{21}$ are summarized in Table 1; the final atomic coordinates in the unit cell and the temperature parameters

Table 3. Interatomic Al–S distances (in Å) and bond angles (in °) with standard deviations for $Tl_3Al_{13}S_{21}$.^a

Al(1)–S(6a)	2.311(10)	S(6a)–Al(1)–S(7a)	104.0(5)	Al(8)–S(15)	2.193(12)	S(15)–Al(8)–S(17b)	121.8(5)
Al(1)–S(7a)	2.197(12)	S(6a)–Al(1)–S(13a)	105.4(4)	Al(8)–S(17b)	2.229(12)	S(15)–Al(8)–S(18)	109.1(4)
Al(1)–S(13a)	2.328(11)	S(6a)–Al(1)–S(19)	110.9(5)	Al(8)–S(18)	2.298(10)	S(15)–Al(8)–S(21b)	106.7(4)
Al(1)–S(19)	2.200(10)	S(7a)–Al(1)–S(13a)	108.9(4)	Al(8)–S(21b)	2.327(10)	S(17b)–Al(8)–S(18)	106.1(4)
		S(7a)–Al(1)–S(19)	114.1(4)			S(17b)–Al(8)–S(21b)	107.0(4)
		S(13a)–Al(1)–S(19)	112.7(4)			S(18)–Al(8)–S(21b)	105.0(4)
Al(2)–S(2)	2.195(9)	S(2)–Al(2)–S(9b)	102.9(4)	Al(9)–S(5)	2.189(10)	S(5)–Al(9)–S(5f)	102.5(5)
Al(2)–S(9b)	2.299(11)	S(2)–Al(2)–S(10)	112.4(5)	Al(9)–S(5f)	2.189(10)	S(5)–Al(9)–S(16)	109.1(4)
Al(2)–S(10)	2.316(11)	S(2)–Al(2)–S(15)	110.8(4)	Al(9)–S(16)	2.310(16)	S(5)–Al(9)–S(22)	113.9(4)
Al(2)–S(15)	2.212(10)	S(9b)–Al(2)–S(10)	109.4(4)	Al(9)–S(22)	2.267(14)	S(5f)–Al(9)–S(16)	109.1(4)
		S(9b)–Al(2)–S(15)	112.4(4)			S(5f)–Al(9)–S(22)	113.9(4)
		S(10)–Al(2)–S(15)	108.5(4)			S(16)–Al(9)–S(22)	108.2(5)
Al(3)–S(8b)	2.305(10)	S(8b)–Al(3)–S(9b)	105.4(4)	Al(10)–S(4)	2.187(11)	S(4)–Al(10)–S(12)	108.0(4)
Al(3)–S(9b)	2.323(10)	S(8b)–Al(3)–S(19)	107.0(4)	Al(10)–S(12)	2.286(10)	S(4)–Al(10)–S(16)	109.0(5)
Al(3)–S(19)	2.196(12)	S(8b)–Al(3)–S(24b)	109.2(4)	Al(10)–S(16)	2.286(10)	S(4)–Al(10)–S(21)	113.8(5)
Al(3)–S(24b)	2.222(12)	S(9b)–Al(3)–S(19)	109.9(4)	Al(10)–S(21)	2.276(12)	S(12)–Al(10)–S(16)	109.2(5)
		S(9b)–Al(3)–S(24b)	104.2(4)			S(12)–Al(10)–S(21)	107.9(4)
		S(19)–Al(3)–S(24b)	120.4(5)			S(16)–Al(10)–S(21)	108.9(4)
Al(4)–S(2)	2.203(12)	S(2)–Al(4)–S(4b)	123.7(4)	Al(11)–S(3)	2.329(10)	S(3)–Al(11)–S(14)	104.6(4)
Al(4)–S(4b)	2.210(13)	S(2)–Al(4)–S(8b)	104.4(5)	Al(11)–S(14)	2.203(11)	S(3)–Al(11)–S(18)	102.1(4)
Al(4)–S(8b)	2.300(12)	S(2)–Al(4)–S(13)	109.7(5)	Al(11)–S(18)	2.300(12)	S(3)–Al(11)–S(24g)	111.1(4)
Al(4)–S(13)	2.315(10)	S(4b)–Al(4)–S(8b)	108.3(5)	Al(11)–S(24g)	2.215(10)	S(14)–Al(11)–S(18)	109.4(4)
		S(4b)–Al(4)–S(13)	103.1(5)			S(14)–Al(11)–S(24g)	116.8(5)
		S(8b)–Al(4)–S(13)	106.8(4)			S(18)–Al(11)–S(24g)	111.8(4)
Al(5)–S(1)	2.233(10)	S(1)–Al(5)–S(3c)	113.2(5)	Al(12)–S(12a)	2.288(11)	S(12a)–Al(12)–S(17)	113.9(4)
Al(5)–S(3c)	2.295(12)	S(1)–Al(5)–S(8)	111.0(4)	Al(12)–S(17)	2.182(10)	S(12a)–Al(12)–S(20a)	107.8(5)
Al(5)–S(8)	2.289(11)	S(1)–Al(5)–S(11)	107.5(5)	Al(12)–S(20a)	2.257(12)	S(12a)–Al(12)–S(22a)	107.4(5)
Al(5)–S(11)	2.209(10)	S(3c)–Al(5)–S(8)	105.8(5)	Al(12)–S(22a)	2.310(10)	S(17)–Al(12)–S(20a)	114.1(5)
		S(3c)–Al(5)–S(11)	108.2(4)			S(17)–Al(12)–S(22a)	105.3(5)
		S(8)–Al(5)–S(11)	111.3(5)			S(20a)–Al(12)–S(22a)	108.0(4)
Al(6)–S(6a)	2.299(16)	S(6a)–Al(6)–S(10)	107.4(5)	Al(13)–S(7a)	2.208(11)	S(7a)–Al(13)–S(11e)	123.4(4)
Al(6)–S(10)	2.287(13)	S(6a)–Al(6)–S(23a)	111.8(4)	Al(13)–S(11e)	2.202(12)	S(7a)–Al(13)–S(18h)	108.5(5)
Al(6)–S(23a)	2.226(10)	S(6a)–Al(6)–S(23d)	111.8(4)	Al(13)–S(18h)	2.310(10)	S(7a)–Al(13)–S(20a)	108.9(5)
Al(6)–S(23d)	2.226(10)	S(10)–Al(6)–S(23a)	110.3(4)	Al(13)–S(20a)	2.329(11)	S(11e)–Al(13)–S(18h)	106.5(4)
		S(10)–Al(6)–S(23d)	110.3(4)			S(11e)–Al(13)–S(20a)	103.0(5)
		S(23a)–Al(6)–S(23d)	105.4(5)			S(18h)–Al(13)–S(20a)	105.1(3)
Al(7)–S(9b)	2.291(10)	S(9b)–Al(7)–S(12e)	100.1(4)	Al(14)–S(3h)	2.273(12)	S(3h)–Al(14)–S(5)	116.3(4)
Al(7)–S(12e)	2.302(12)	S(9b)–Al(7)–S(13a)	106.5(4)	Al(14)–S(5)	2.179(12)	S(3h)–Al(14)–S(20)	102.6(4)
Al(7)–S(13a)	2.274(12)	S(9b)–Al(7)–S(23a)	115.4(5)	Al(14)–S(20)	2.300(10)	S(3h)–Al(14)–S(21)	102.2(4)
Al(7)–S(23a)	2.177(12)	S(12e)–Al(7)–S(13a)	104.0(5)	Al(14)–S(21)	2.291(11)	S(5)–Al(14)–S(20)	114.4(5)
		S(12e)–Al(7)–S(23a)	112.8(4)			S(5)–Al(14)–S(21)	113.9(5)
		S(13a)–Al(7)–S(23a)	116.3(5)			S(20)–Al(14)–S(21)	106.0(4)

^aa (x, y, 1+z); b (1/2+x, 1/2–y, z); c (x–1, y, z); d (x, –y, 1+z); e (1/2+x, 1/2–y, 1+z); f (x, –y, z); g (1+x, y, z); h (x–1/2, 1/2–y, z); i (x–1/2, y–1/2, z); j (x, y, z–1); k (x, –y, z–1); l (1/2+x, y–1/2, z); m (1+x, y, 1+z); n (1+x, –y, 1+z); o (1/2+x, y–1/2, 1+z); p (x–1/2, 1/2+y, z); q (x–1/2, 1/2+y, 1+z); r (x–1/2, 1/2–y, 1+z).

are given in Table 2. Interatomic distances and bond angles are listed in Tables 3 and 4.*

* A list of observed and final calculated structure factors and further details of the structure (anisotropic temperature factors, bond angles at Tl and non-bonded distances) is available from the Fachinformationszentrum Energie, Physik, Mathematik GmbH, D-7514 Eggenstein-Leopoldshafen, by quoting the depository number CSD 55188, the names of the authors and the citation of the journal.

Description of the structure and discussion

The anionic polymeric part of the structure is built up of slightly distorted $[AlS_4]$ tetrahedra connected only by common corners creating a three-dimensional network. The ratio of μ_3 [S(3), S(6), S(8), S(9), S(10), S(12), S(13), S(16), S(18), S(20), S(21), S(22)] and μ_2 [S(1), S(2), S(4), S(5), S(7), S(11), S(14), S(15), S(17), S(19), S(23), S(24)] sulfur atoms is 12 to 12. Six-, eight- and twelve-membered $[Al_3S_3]$, $[Al_4S_4]$, and $[Al_6S_6]$ rings are formed. The structure

Table 4. Interatomic Tl-S distances (in Å) for $Tl_3Al_{13}S_{21}$.

Tl(1)-S(1)	3.316(11)	Tl(3)-S(5f)	3.532(8)	Tl(5)-S(11m)	3.436(8)
Tl(1)-S(4)	3.710(7)	Tl(3)-S(6)	3.719(11)	Tl(5)-S(11n)	3.436(8)
Tl(1)-S(4f)	3.710(7)	Tl(3)-S(7)	3.693(7)	Tl(5)-S(14)	3.164(11)
Tl(1)-S(11)	3.280(8)	Tl(3)-S(7f)	3.693(7)	Tl(5)-S(15)	3.266(7)
Tl(1)-S(11f)	3.280(8)	Tl(3)-S(8l)	3.729(8)	Tl(5)-S(15f)	3.266(7)
Tl(1)-S(13i)	3.806(8)	Tl(3)-S(8b)	3.729(8)	Tl(5)-S(20o)	3.829(9)
Tl(1)-S(13h)	3.806(8)	Tl(3)-S(10)	3.633(9)	Tl(5)-S(20e)	3.829(9)
Tl(1)-S(24j)	3.484(7)	Tl(3)-S(19)	3.537(8)	Tl(5)-S(23a)	3.746(9)
Tl(1)-S(24k)	3.484(7)	Tl(3)-S(19f)	3.537(8)	Tl(5)-S(23d)	3.746(9)
Tl(2)-S(1)	3.109(9)	Tl(4)-S(5)	3.555(8)	Tl(6)-S(2)	3.493(9)
Tl(2)-S(4)	3.229(8)	Tl(4)-S(5f)	3.555(8)	Tl(6)-S(2f)	3.493(9)
Tl(2)-S(4f)	3.229(8)	Tl(4)-S(7a)	3.431(7)	Tl(6)-S(3)	3.974(8)
Tl(2)-S(9)	3.768(7)	Tl(4)-S(7d)	3.431(7)	Tl(6)-S(3f)	3.974(8)
Tl(2)-S(9f)	3.768(7)	Tl(4)-S(16)	3.902(9)	Tl(6)-S(14)	3.544(9)
Tl(2)-S(17)	3.881(8)	Tl(4)-S(17)	3.672(8)	Tl(6)-S(15)	3.272(8)
Tl(2)-S(17f)	3.881(8)	Tl(4)-S(17f)	3.672(8)	Tl(6)-S(15f)	3.272(8)
Tl(2)-S(24)	3.581(8)	Tl(4)-S(18i)	3.789(8)	Tl(6)-S(21)	3.767(9)
Tl(2)-S(24f)	3.581(8)	Tl(4)-S(18h)	3.789(8)	Tl(6)-S(21b)	3.767(9)
Tl(3)-S(2)	3.455(9)	Tl(4)-S(19)	3.503(9)	Tl(6)-S(23)	3.687(8)
Tl(3)-S(2f)	3.455(9)	Tl(4)-S(19f)	3.503(9)	Tl(6)-S(23f)	3.687(8)
Tl(3)-S(5)	3.532(8)	Tl(4)-S(22a)	3.708(11)		

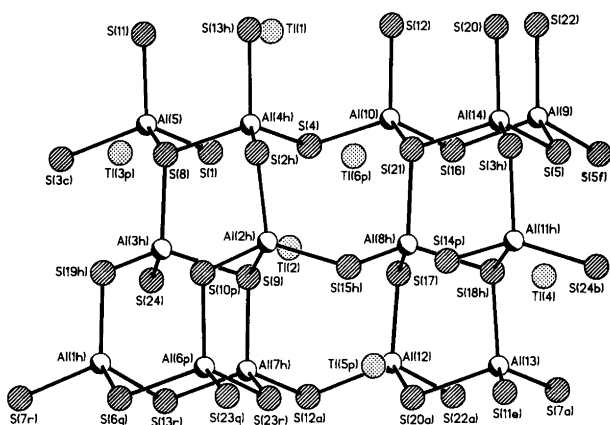


Fig. 1. Topological diagram of the structure of $Tl_3Al_{13}S_{21}$ with atomic designations, illustrating the connection of the $[AlS_4]$ tetrahedra. The projection of the picture is approximately along $[100]$. The indices to the atomic numbers refer to the transformations given in Table 3.

also contains "open adamantane"-like species lacking only one Al-S pair compared to an $[Al_4S_{10}]$ adamantane (Fig. 1).

The Tl^+ ions are found in tunnels running along $[001]$ (Fig. 2). The diameter of the tunnels is defined by 12-membered $[Al_6S_6]$ rings perpendicular to the tunnel direction which are also found in the structure of $BaAl_4S_7$.¹³ Along their axes the tunnels are bounded by eight-membered $[Al_4S_4]$ and six-membered $[Al_3S_3]$ rings, leading to a rather open framework around the thallium cations.

As an alternative description, the polymeric anionic arrangement of corner-sharing $[AlS_4]$ tetrahedra may be considered as an ... AABAAB ... ordering of defect tetra-

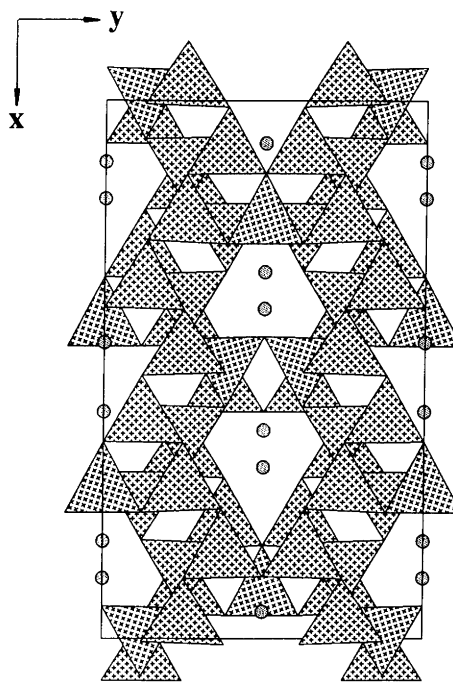


Fig. 2. $Tl_3Al_{13}S_{21}$: Projection of the structure along $[001]$ (polyhedral representation; dotted spheres, Tl).

hedral layers running perpendicular to c (Fig. 3). In other words, two layers of a defect zincblende type are followed by a defect layer with the rotated (wurtzite-like) orientation of the $[AlS_4]$ tetrahedra. In a packing picture, the overall structure can be described as a distorted close packing of $21 S + 3 Tl$ per formula unit, with an ordered occupation of 13 of the tetrahedral voids by Al.

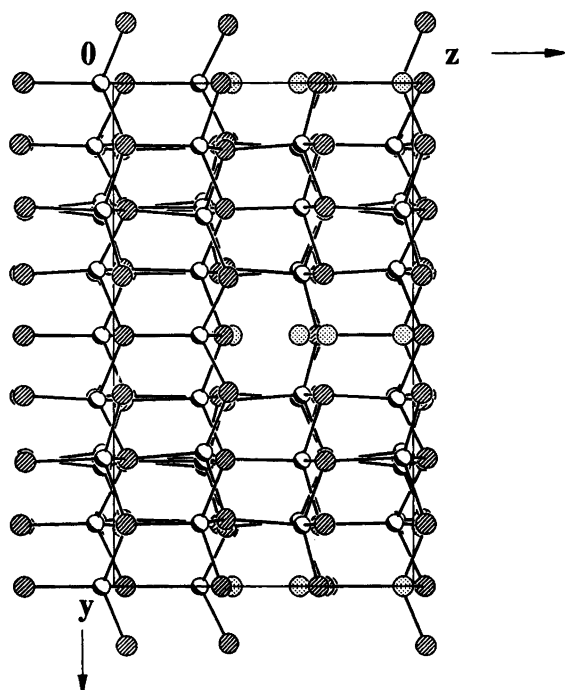


Fig. 3. [100] projection of the $\text{Th}_3\text{Al}_{13}\text{S}_{21}$ structure (dotted, Tl; shaded, Al; hatched, S).

Within the distorted close packing 14 of the sulfur atoms in the asymmetric unit [S(1), S(2), S(3), S(4), S(5), S(7), S(11), S(12), S(14), S(15), S(17), S(19), S(23), S(24)] are in

contact with $10\text{S} + 2\text{Tl}$; the remaining 10 sulfur atoms [S(6), S(8), S(9), S(10), S(13), S(16), S(18), S(20), S(21), S(22)] have $11\text{S} + 1\text{Tl}$ close-packed neighbours. The $\text{S}\cdots\text{S}$ contacts range from 3.414(17) to 3.935(17) Å, while the $\text{S}\cdots\text{Tl}$ distances are from 3.109(9) to 4.294(7) Å.

The coordination of the thallium atoms by the bonded sulfur atoms is shown in Fig. 4. All Tl atoms are on special positions 2a with site symmetry m . If the distances below 4 Å are counted as being significantly bonding, the thallium atoms are coordinated symmetrically by 12 [Tl(3), Tl(4)], 11 [Tl(6)] or 9 sulfur atoms [Tl(1), Tl(2), Tl(5)]. All coordination polyhedra are more or less irregular (Fig. 4) owing to the stereochemical activity of the lone pairs at Tl. This effect is especially pronounced for the nine-coordinated Tl(1), Tl(2) and Tl(5) with six sulfur ligands in an equatorial position and the remaining three sulfur atoms coordinated asymmetrically on one side of the equatorial plane. The higher coordination numbers of the other three Tl atoms show increasing Tl-S distances and decreasing asymmetry of the bonding pattern. The rather long Tl-S distances in the structure of $\text{Th}_3\text{Al}_{13}\text{S}_{21}$ (Table 4) are typical of highly coordinated Tl^+ with rather ionic Tl-S bonding, as compared to the more covalent Tl-S bonds in low-coordinate polyhedra, e.g. in the $[\text{TlS}_3]$ units of thallium thioalates,¹⁴ which have mean values of 2.92–3.17 Å. The Tl-S coordination polyhedra in $\text{Th}_3\text{Al}_{13}\text{S}_{21}$ are very similar to those found in $\text{Tl}_4\text{Sn}_5\text{S}_{12}$,⁸ for which two categories of Tl-S distances are discussed, ranging between the calculated ionic and the van der Waals distance. The shortest Tl \cdots Tl contacts in the structure of $\text{Th}_3\text{Al}_{13}\text{S}_{21}$ are 4.558(3) Å for

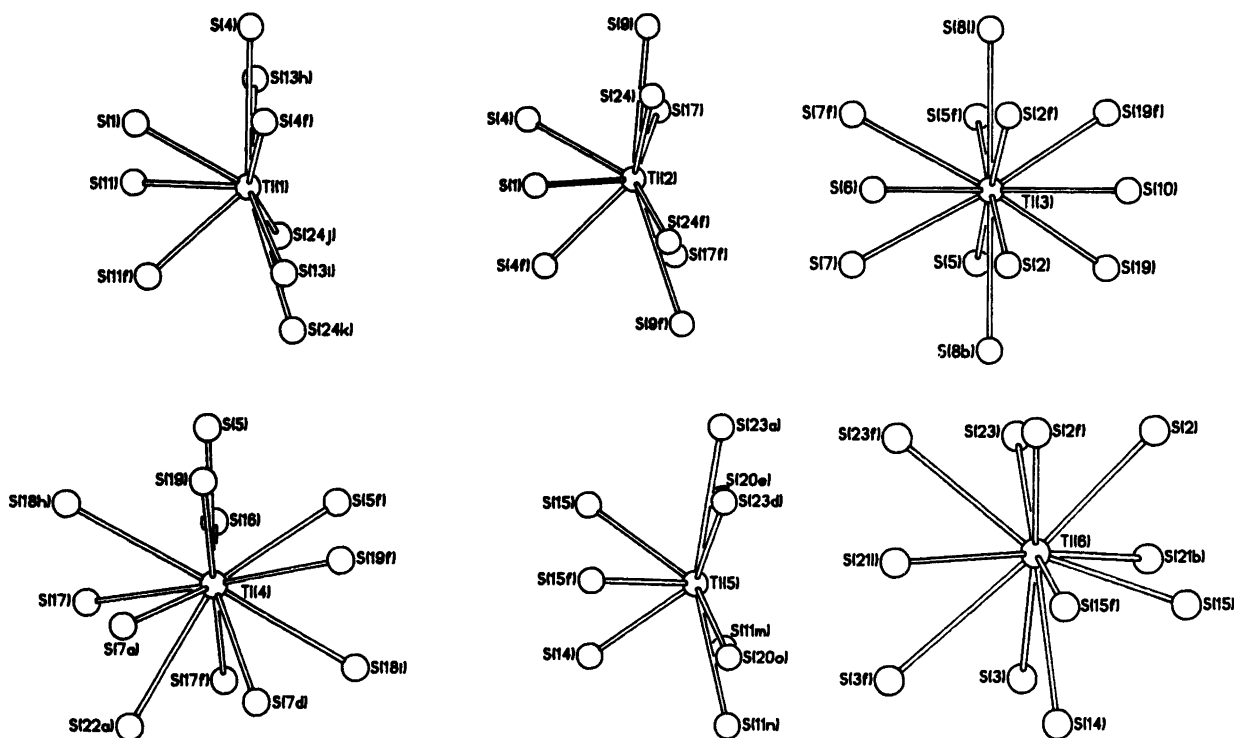


Fig. 4. Thallium-sulfur coordination in the crystal structure of $\text{Th}_3\text{Al}_{13}\text{S}_{21}$.

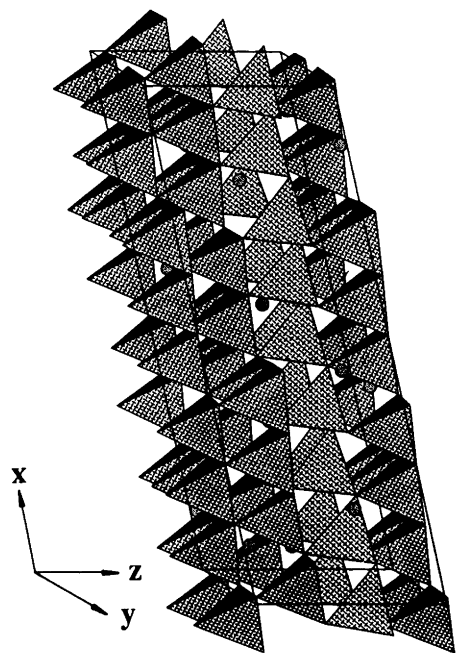


Fig. 5. Polyhedral representation of the unit cell of $Tl_3Al_{13}S_{21}$ (dotted spheres, Tl).

$Tl(1) \cdots Tl(2j)$, 5.042(4) Å for $Tl(3) \cdots Tl(4)$ and 4.720(4) Å for $Tl(5) \cdots Tl(6a)$, so that weak Tl–Tl attractive interactions are unlikely.

The Al–S distances, ranging from 2.177 to 2.329 Å (Table 3), are comparable with those found in other Al–S compounds, with significant Al–S bond elongation for the Al– μ_3 S bonds (mean Al– μ_3 S distance 2.296 Å, mean Al– μ_2 S distance 2.203 Å). All $[AlS_4]$ tetrahedra are slightly distorted and show deviations from the ideal tetrahedral angles (Table 3). This, however, is not surprising if the large steric constraints by the polymeric framework and the distorting influence of the Tl^+ are taken into account.

There are interesting structural relationships between $Tl_3Al_{13}S_{21}$ and the tetrahedral forms of binary Al_2S_3 . At normal pressure Al_2S_3 is known to form three polymorphs:^{15–18} a hexagonal α -form (ordered-defect wurtzite type), a hexagonal β -form (disordered-defect wurtzite type) and a hexagonal rhombohedral γ -form having the corundum structure. The hexagonal close packing of sulfur appearing in α - and β - Al_2S_3 can be compared to the close packing of 21 S + 3 Tl in the structure of $Tl_3Al_{13}S_{21}$, here, however, being distorted as a result of the stereochemical activity of the lone electron pair of Tl^+ . Within the crystal structure of $Tl_3Al_{13}S_{21}$ one can distinguish between closer packed (more highly condensed) $[AlS_4]$ tetrahedra in the Al-rich polyanionic domains and a less dense framework of $[AlS_4]$ tetrahedra around the tunnels along [001] coordinating the Tl^+ ions (Fig. 5). Considering these structural features, interesting physical properties, in particular with respect to possible anisotropic or non-linear electrical or optical properties and low-temperature phase transitions, can be expected.

In the recent literature a study of the ferroelectric phase transition of $TlGaSe_3$ ^{19,20} observed at low temperature is reported. According to the authors of Refs. 19 and 20 the ferroelectricity is strongly related to the lone-pair configuration of the Tl^+ ion, with a physically relevant loss of symmetry resulting from small positional shifts of the Tl atoms. This might also be true for the structure of $Tl_3Al_{13}S_{21}$; a phase transition at low temperature seems to be present, as indicated from preliminary results. Further investigations are in progress.

The crystal structures of $ZnAl_2S_4$ ^{21,22} (with much higher symmetries, however) are another example of a low-temperature–high-temperature phase transition in ternary systems based on aluminium sulfide. Here the low-temperature α - $ZnAl_2S_4$ (normal spinel structure type) and the high-temperature β - $ZnAl_2S_4$ (defect wurtzite with Zn and Al randomly distributed amongst three quarters of the tetrahedral sites) are realized.

Finally, comparing $TlAlS_2$, the only phase so far known in the Tl_2S/Al_2S_3 system, to the structure of $Tl_3Al_7S_{12}$, it is evident that the degree of polymerization of the $[AlS_4]$ tetrahedra can be controlled by variation of the Tl_2S/Al_2S_3 ratio. Our most recent work, which led to the discovery of further novel and unexpected phases in this system,¹¹ confirms this concept: Tl_3AlS_4 contains isolated $[AlS_4]$ tetrahedra without Al–S–Al bridging, and $Tl_3Al_7S_{13}$ shows a complicated three-dimensionally polymeric anion framework of composition $[Al_7S_{12}^{3-}]_n$ with a ratio of 4:8 for μ_3 and μ_2 bridging sulfur atoms.¹¹ The remarkable mixed-valence compound Tl_xAlS_2 ($x \approx 0.5$) crystallizes in a TlSe-type structure with defects in the square antiprismatically coordinated metal site.¹¹ Further work is in progress.

Acknowledgements. The authors are grateful to Mrs. M. Dartmann for valuable experimental help. They also thank the *Deutsche Forschungsgemeinschaft* and the *Fonds der Chemischen Industrie* for financial support.

References

- Hellstrom, E. E. and Huggins, R. A. *Mater. Res. Bull.* 14 (1979) 881.
- Krebs, B. and Hamann, W. *J. Less-Comm. Met.* 137 (1988) 143.
- Krebs, B. *Angew. Chem.* 95 (1983) 113; *Angew. Chem., Int. Ed. Engl.* 22 (1983) 113.
- Eulenberger, G. *Acta Crystallogr., Sect. C* 42 (1986) 528.
- Eulenberger, G. *Monatsh. Chem.* 113 (1982) 859.
- del Bucchia, S., Jumas, J. C., Philippot, E. and Maurin, M. *Rev. Chim. Miner.* 18 (1981) 224.
- Ajavon, A.-L., Eholie, R., Piffard, Y. and Tournoux, M. *Rev. Chim. Miner.* 20 (1983) 421.
- Ajavon, A.-L., Eholie, R., Piffard, Y. and Tournoux, M. *Rev. Chim. Miner.* 21 (1984) 56.
- Müller, D. and Hahn, H. *Z. Anorg. Allg. Chem.* 438 (1978) 258.
- Janssen, H. *Doctoral Thesis*, University of Münster, Germany 1985.

11. Krebs, B., Greiwing, H. and Janssen, H. *To be published.*
12. Eisenmann, B., Jakowski, M. and Schäfer, H. *Mater. Res. Bull.* 17 (1982) 1169.
13. Eisenmann, B., Jakowski, M. and Schäfer, H. *Rev. Chim. Miner.* 20 (1983) 329.
14. Krebs, B. and Brömmelhaus, A. *Angew. Chem.* 101 (1989) 1726; *Angew. Chem., Int. Ed. Engl.* 28 (1989) 1682.
15. Flahaut, J. C. R. *Hebd. Acad. Sci.* 232 (1951) 334.
16. Flahaut, J. C. R. *Hebd. Acad. Sci.* 232 (1951) 2100.
17. Flahaut, J. *Ann. Chim.* 7 (1952) 632.
18. Hellstrom, E. E. and Huggins, R. A. *Mater. Res. Bull.* 14 (1979) 127.
19. Hochheimer, H. D., Gmelin, E., Bauhofer, W., von Schnering-Schwarz, Ch., von Schnering, H. G., Ihringer, J. and Appel, W. *Z. Phys. B.* 73 (1988) 257.
20. Henkel, W., Hochheimer, H. D., Carlone, C., Werner, A., Ves, S. and von Schnering, H. G. *Phys. Rev. B* 26 (1982) 3211.
21. Steigmann, G. A. *Acta Crystallogr.* 23 (1967) 142.
22. Hahn, H. and Frank, G. *Z. Anorg. Allg. Chem.* 269 (1952) 227.

Received December 18, 1990.